(11) Galin, M.; Rupprecht, M. C. *Polymer* **1978**, *19*, 506.
(12) Hu, D. S.; Han, C. D.; Stiel, L. I. *J. Appl. Polym. Sci.* **1987**, *33*, 551.
(13) Munk, P.; Card, C. W.; Hattam, P.; El-Hibri, M. J.; Al-Saigh, Z. Y. *Macromolecules* **1987**, *20*, 1278.
(14) Vrentas, J. S.; Duda, J. L. *J. Polym. Sci., Polym. Phys. Ed.* **1977**, *15*, 441.
(15) Pawlisch, C. A. Ph.D. Dissertation, University of Massachusetts at Amherst, 1985.
(16) Ramachandran, P. A.; Smith, J. M. *Ind. Eng. Chem. Fundam.* **1978**, *17*, 148.
(17) Radeke, K. H. *Ind. Eng. Chem. Fundam.* **1981**, *20*, 302.
(18) Haynes, H. W. *Chem. Eng. Sci.* **1975**, *30*, 955.
(19) Boersma-Klein, W.; Moulijn, J. A. *Chem. Eng. Sci.* **1978**, *34*, 959.
(20) Johnson, J. L.; Fan, L. T.; Wu, Y. S. *Ind. Eng. Chem. Process Des. Dev.* **1971**, *10*, 425.
(21) Hays, J. R.; Clements, W. C. Jr.; Harris, T. R. *AIChE J.* **1967**, *13*, 375.
(22) Dahlquist, G.; Bjorck, A. *Numerical Methods*; Prentice Hall: Englewood Cliffs, NJ, 1974.
(23) Weinberger, H. F. *A First Course in Partial Differential Equations*; Wiley: New York, 1965.
(24) Vrentas, J. S.; Duda, J. L. *J. Appl. Polym. Sci.* **1978**, *22*, 2325.
(25) Hu, D. S.; Han, C. D. *J. Appl. Polym. Sci.* **1987**, *34*, 423.
(26) Zhurkov, S. N.; Ryskin, G. V. *Zh. Tekh. Fiz.* **1954**, *24*, 797.
(27) Hopfenberg, H. B.; Stannett, V. T.; Jacques, C. H. M. *J. Appl. Polym. Sci.* **1975**, *19*, 2485.
(28) Wang, T. T.; Kwei, T. K. *Macromolecules* **1973**, *6*, 919.
(29) Berens, A. R.; Hopfenberg, H. B. *J. Membr. Sci.* **1982**, *10*, 283.
(30) Vrentas, J. S.; Duda, J. L.; Hsieh, S. T. *Ind. Eng. Chem. Prod. Res. Dev.* **1983**, *22*, 326.

Anomalous Small-Angle X-ray Scattering from a Sulfonated Polystyrene Ionomer

Y. Samuel Ding,[†,§] Stevan R. Hubbard,[‡,⊥] Keith O. Hodgson,[‡] Richard A. Register,[†] and Stuart L. Cooper*[,†]

Department of Chemical Engineering, University of Wisconsin—Madison, Madison, Wisconsin 53706, and Departments of Chemistry and Applied Physics, Stanford University, Stanford, California 94305. *Received September 1, 1987; Revised Manuscript Received December 2, 1987*

ABSTRACT: Anomalous small-angle X-ray scattering has been employed to study the morphology of a nickel-neutralized sulfonated polystyrene ionomer, with particular emphasis on the characteristic upturn in scattered intensity near zero angle. The results indicate that the zero-order scattering is related to the ionomer's neutralizing cation. Applying the Debye–Bueche random two-phase model to the data indicates that the heterogeneity giving rise to the zero-angle scattering has a much larger length scale and smaller electron density difference than the aggregate–matrix scattering and may be due to an inhomogeneous distribution of isolated ionic groups in the matrix.

I. Introduction

Small-angle X-ray scattering (SAXS) has been shown to be a powerful technique for characterizing the morphology of ionomers,[1-10] but to correlate SAXS results with the physical, chemical, or transport properties, ionomer morphology must be understood. Typical ionomer SAXS patterns contain a peak with a Bragg spacing typically 20–100 Å and a strong upturn in intensity as zero angle is approached. The peak has been taken as a signature of ionic aggregation since it was first observed,[1] and numerous SAXS studies have established the validity of this assignment.[1-10] But while several detailed ionomer morphological models have been proposed,[9,10] none can fit both the peak and the upturn with a consistent set of parameters. As a result, Yarusso and Cooper[10] have suggested that the upturn might be artifactual, possibly arising from residual camera scattering or impurities or voids in the samples. Recent work by Kumar and Pinéri[8] shows that scattering from a uniformly electron dense but finite sample volume gives an upturn qualitatively similar to that observed in ionomers. However, the calculated intensity from this source is considerably smaller than what is observed, meaning that an additional source of scattered intensity must exist.

To determine whether the cations in the ionomer give rise to the observed upturn as well as peak scattering, it would be highly desirable to separate scattering involving the cation from nonionic scattering sources. Selectively changing the scattering power of one of the scattering elements in a material has been widely used for this purpose in mineral and biological crystallography. One often-used method is to prepare a second material which has the same structure as the one under study, but with one type of atom replaced with one much lighter or heavier (known as an isomorphous derivative); however, this procedure suffers from the difficulty of producing two samples of identical morphology.[11] Another means of varying scattering contrast is to perform a set of complementary scattering experiments (X-ray, neutron, electron) on a single sample,[12] but a single sample is generally unsuitable for more than one type of experiment. Recently, with the availability of intense, continuously tunable X-rays from synchrotron sources, anomalous small-angle X-ray scattering (ASAXS) has been demonstrated as a uniquely powerful method for changing the scattering contrast of a selected element.[11,13-19] This paper describes the application of ASAXS to a nickel-neutralized sulfonated polystyrene ionomer.

II. Experimental Section

A. Sample Preparation. The sulfonated polystyrene studied was obtained from Dr. Robert Lundberg and the late Dr. Henry Makowski of the Exxon Research and Engineering Co. and was

* To whom correspondence should be addressed.
† University of Wisconsin—Madison.
‡ Stanford University.
§ Present address: Baxter Healthcare Corporation, Round Lake, IL 60073.
⊥ Present address: Department of Biochemistry and Molecular Biophysics, College of Physicians and Surgeons of Columbia University, New York, NY 10032.

0024-9297/88/2221-1698$01.50/0

prepared by procedures described elsewhere.[20,21] The chemical structure of sulfonated polystyrene is

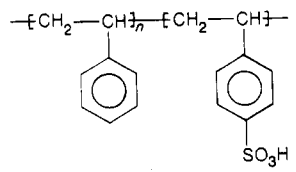

For the sample used in this study, 5.6 mol % of the styrene units were sulfonated, as determined by atomic absorption analysis, so the average value of n in the random copolymer is about 17. To prepare the nickel ionomer, a 5 wt % solution of the acid form shown above was prepared in tetrahydrofuran and passed through filter paper under nitrogen pressure. The filtered solution was then neutralized with an aqueous solution of nickel acetate tetrahydrate and was stirred for 2 h at 60 °C. The volumetric ratio between the miscible aqueous and polymer solutions was 1:9. Only 95% of the stoichiometric amount of nickel was added to minimize the possibility that residual nickel acetate would be trapped in the polymer.

After neutralization, the polymer was recovered by pouring the solution into 80 °C distilled water, with vigorous stirring. The polymer precipitated as a floc and was washed with 80 °C distilled water several times in order to remove any unreacted nickel acetate. The polymer was then vacuum-dried at 80 °C for 48 h and then at 120 °C for 24 h, followed by slow cooling under vacuum over a period of 4 h to room temperature. A suitable sample for ASAXS experiments was prepared by compression molding the nickel ionomer into a 1-mm-thick disk, at 180 °C and 8000 psi for 10 min.

B. ASAXS Measurements. ASAXS experiments were conducted on Beamline II-2 at the Stanford Synchrotron Radiation Laboratory (SSRL). X-ray energies 5 and 100 eV below the measured K edge for Ni^{2+} in the ionomer (8333 eV in Ni metal) were selected by a double-crystal monochromator using planar Si(111) crystals with a nominal resolution of ±4 eV. The scattering apparatus comprised a He/N_2-filled ionization chamber for incident beam monitoring, an evacuated sample-to-detector tube, and a one-dimensional Ar-filled position-sensitive detector. The integral linearity of the detector was better than 3%. The stop for the primary beam was a wedge coated with ZnS; the fluorescent intensity from the ZnS was monitored by a photodiode within the beamstop assembly. The X-rays were collimated by two sets of slits: one set just in front of the monochromator and the other set just in front of the ionization chamber. A third set of slits placed after the ionization chamber and before the sample holder minimized parasitic scattering. The spot size at the sample position was approximately 400 × 400 μm. A mask with a 2.65-mm-wide slit was used at the detector to decrease "smearing" of the ASAXS patterns. A more complete description of the apparatus can be found elsewhere.[22]

The data were corrected for transmittance of the sample and fluctuations in incident beam intensity by normalizing the scattered counts to the counts measured by the photodiode. No correction for background scattering was made, as this is automatically canceled between the spectra taken at different energies, as described in the next section. Corrections for dark current and detector sensitivity between pixels were found to be unnecessary. No correction for any change in overall detector sensitivity between the two incident X-ray energies was applied, as the two energies differ by only slightly more than 1%. All data shown herein are on a relative, but consistent, intensity scale.

III. Anomalous Scattering Background[13]

The intensity of X-rays scattered from an object can be expressed as

$$I/I_e = \sum_i \sum_j f_i f_j^* e^{-i\mathbf{q}(\mathbf{r}_i - \mathbf{r}_j)} \quad (1)$$

where the scattering vector magnitude $q = (4\pi/\lambda) \sin \theta$, 2θ is the scattering angle, I_e is the intensity scattered by a single electron, and $\mathbf{r}_i$ and $\mathbf{r}_j$ are the position vectors of two scattering entities within the object. In general, the atomic form factors f are both energy dependent and complex, as expressed by

$$f = f_0 + f'(E) + if''(E) \quad (2)$$

where f_0 is energy-independent. The anomalous dispersion terms f' and f'' are small compared with f_0 at most energies, but at energies close to an atomic absorption edge, they can become significant, as much as 30% of f_0. The f' term becomes increasingly negative as an absorption edge is approached from lower energy, which causes the scattered X-ray intensity to diminish near the edge. The f'' term is equal to $E\mu(E)$, where $\mu(E)$ is the X-ray absorption coefficient;[23] as such, f'' is small at energies below the edge, but at the edge it jumps sharply and then decreases as the energy is further increased. The two terms are connected through the Kramers–Kronig relations.[24,25] As all our measurements were conducted below the absorption edge, we will concern ourselves only with the effect of f', except in correcting for fluorescence as described below.

Values of f' for Ni have been determined experimentally in several ways, in addition to theoretical calculations.[15] Recent high-precision studies have employed direct measurement of f' via X-ray interferometry[23] of Ni foil, measurement of f'' on Ni foil[23] and application of the Kramers–Kronig relations, and absolute intensity measurements of crystal reflections[26] in powdered Ni. Results from the three methods are essentially in agreement and indicate that f' is approximately −3.8 electrons (out of 28 total electrons for Ni) at 100 eV below the edge, while being approximately −6.7 electrons at 5 eV below the edge. This corresponds to a 23% change in scattered intensity between the two energies, which is easily discernible. Although the f' values depend on the valence state and chemical environment of the absorbing cation, the large anomalous effect observed for nickel foil suggests that the effect will also be observable for the nickel ionomer.

Scattered intensity for an ionomer can be expressed as

$$I = I_{\text{aggregates}} + I_{\text{background}} \quad (3)$$

where

$$I_{\text{background}} = I_{\text{crystals}} + I_{\text{voids}} + I_{\text{impurities}} + I_{\text{amorphous halo}} + \dots \quad (4)$$

This separation of the total scattering into parts arising from different types of scattering centers in the material is valid when there is no positional correlation between the different entities. In general, the background scattering does not contain any contribution from the cation, the only possible exception being a cation-containing impurity, such as precipitated neutralizing agent in an over-neutralized ionomer.

If the background scattering does not contain a cation contribution, then its intensity should be independent of energy. In contrast, scattering centers containing the cation will have their scattering power changed as the X-ray energy is tuned near the cation's absorption edge. Therefore, if two scattering patterns are collected, one at an energy E_1 far from the cations's absorption edge and one at an energy E_2 close to the edge, subtraction of the two patterns will yield a "difference pattern" reflecting only the scattering involving cation-containing entities:

$$I(E_1) - I(E_2) = \Delta I_{\text{exptl}} = \Delta I_{\text{cations}} \quad (5)$$

When working near the absorption edge, however, fluorescent X-rays will also be generated in the sample and contribute to the observed scattering intensity. The fluorescent X-rays arise from the finite energy band-pass of the monochromator, such that a small fraction of the

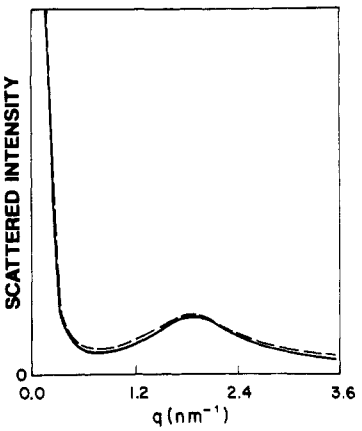

Figure 1. SAXS patterns for nickel-neutralized sulfonated polystyrene at 100 (—) and 5 eV (- - -) below the measured nickel K edge. Relative intensity scale.

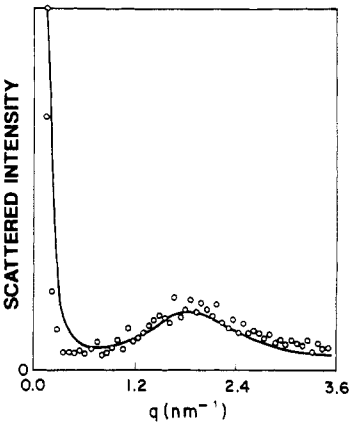

Figure 2. SAXS patterns for nickel-neutralized sulfonated polystyrene at 100 eV (—) below the edge and difference pattern of curves shown in Figure 1 (circles). Difference pattern has been scaled to equal the solid curve in integrated intensity.

passed radiation has an energy above the edge. Using the known angular dependence of the fluorescent radiation,[27] we calculate that the intensities of Ni Kα and Kβ X-rays generated in our sample are independent of angle to within 0.03% over the small angular range used in the ASAXS experiment (roughly 2.5°). Therefore, fluorescence merely appears as a constant upward shift in the scattering pattern collected close to the edge. The fluorescent contribution was estimated by matching the high-q portions of the scattering patterns, beyond the ionomer peak, where the anomalous effects should be small. This contribution was then subtracted from the data. The final equation of interest is

$$\Delta I_{\text{exptl}} - \Delta I_{\text{fluoresc}} = \Delta I_{\text{cations}}(f') \qquad (6)$$

where the term on the right represents the scattering pattern arising from interactions involving only the cation.

While in this paper we address only the amorphous sulfonated polystyrene, it should be pointed out that ASAXS offers an excellent way to separate ionic and crystallite scattering in semicrystalline polymers, such as ethylene/methacrylic acid salts and perfluorinated ionomers; because of the small crystallite size in these materials, the ionic and crystallite scattering peaks overlap, making analysis of either difficult.[6,7] We will pursue this in a later paper.

IV. Results and Discussion

The scattering patterns of the nickel-neutralized sulfonated polystyrene ionomer, taken 5 and 100 eV below the measured cation absorption edge, are shown in Figure 1. By looking at the difference between these two on either side of the ionomer peak, we can see the effect of the constant shift due to fluorescence; once this component is subtracted, the ionomer peak has a lower peak intensity at 5 eV below the edge than at 100 eV below the edge. This demonstrates the anomalous effect discussed in section III. The difference pattern is shown in Figure 2, as well as the pattern 100 eV below the edge. To make visualization easier, the difference pattern has been scaled to equal the raw data in integrated intensity, which entailed multiplication by a factor of 12.5. Therefore, the anomalous effect is 8% of the total intensity for the nickel-neutralized ionomer, as compared with 23% for pure Ni metal. In addition to the variation of f' with valency and chemical environment, the observed magnitude of the anomalous effect is also affected by the fact that the ionic aggregates are not pure Ni^{2+}; they are also expected to contain sulfonate groups, which have a higher electron density than the polystyrene matrix. Scattering between two sulfonate groups would not exhibit any anomalous effect at the nickel edge and would thus contribute to the total scattering but not to the difference pattern; scattering betwen nickel and sulfonate groups would exhibit an anomalous effect, but a weaker one than scattering between two nickel groups. Therefore, we consider the 8% value reasonable.

It should be pointed out that in correcting for fluorescence we have subtracted only a portion of the fluorescent contribution to the observed intensity in order to make the scaled difference pattern resemble the original data in the tail region, which is equivalent to comparing the data sets with background subtracted. However, the noise level in the data, as well as omission of the correction for detector response with incident X-ray energy, makes an accurate determination of the magnitude of the anomalous effect difficult. We have recently acquired ASAXS data on some ionomer systems at multiple energies, which will allow better determination of the magnitude of the anomalous effect and a comparison with f'. These results will be presented in a future paper.

An important fact can be gleaned simply from observation of Figure 2: the upturn in scattered intensity near zero angle is still present, indicating that it must be related to the neutralizing cation. As discussed in section III, if it were from a source devoid of cation, it would have canceled out when the difference pattern was computed. Note also that the ionomer peak is present in the difference pattern and appears similar to that in the original data. This simply confirms the generally accepted postulate that the ionomer peak reflects scattering from the ionic aggregates, which necessarily involves the cation. The relatively high noise level in the difference pattern, the result of taking a small difference of two large quantities, precludes firm conclusions regarding subtle changes in the shape of the scattering pattern, however.

Having established the qualitative appearance of the difference pattern, we now attempt to quantify the data with two different morphological models, both of which have been previously applied to SAXS data from ionomers.[10] Both attribute the ionomer peak to scattering between aggregates, rather than single-particle scattering reflecting intraaggregate structure.[9] The first model describes a simple cubic paracrystal[10,28] with fluctuations in the basis vector lengths, known as disorder of the second kind. The paracrystalline model has as its primary advantage that it predicts both a peak and an upturn. The root-mean-square fluctuation, s, can be compared with the basis vector length, a, to give an indication of the degree of disorder in the paracrystal. Values of the aggregate

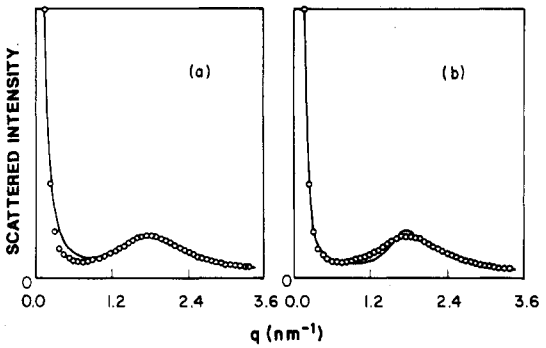

Figure 3. Paracrystalline model fits to SAXS pattern taken 100 eV below the nickel K edge. (a) Best fit for $0.9 < q < 3.5$ nm^{-1}; (b) best fit for $0.2 < q < 3.5$ nm^{-1}. Solid line is the fit; circles are data.

Table I
Paracrystalline Model Fit Parameters[a]

scattering pattern	a, nm	s, nm	R, nm	ρ_1	fit range in q, nm^{-1}
original (100 eV below	3.52	0.94	0.88	13.0	0.9–3.5
edge	3.49	0.77	0.93	11.3	0.2–3.5
difference[b]	3.66	0.99	0.73	23.7	0.9–3.5
	3.89	0.84	0.69	28.1	0.2–3.5

[a] Relative values for ρ_1, as discussed in text. [b] Difference pattern scaled to match original pattern in integrated intensity.

radius R and ρ_1, the electron density difference between the aggregates and the matrix, are also obtained. Since the scattering patterns in this investigation were not converted to absolute intensities by comparison with a calibrated standard, the ρ_1 magnitudes are not meaningful, but comparison of different ρ_1 values does accurately reflect changes in electron density difference.

The second model used is a modified Yarusso (liquid-like) model[10] wherein the Percus–Yevick[29] total correlation function, as solved by Wertheim[30] and Thiele,[31] was used instead of the Fournet[32] three-body type originally employed. Kinning and Thomas[33] have shown that the Percus–Yevick function yields better results than the Fournet function for diblock copolymers exhibiting spherical morphology. The ionic aggregates in this model have an ionic core radius R_1 but are coated with an impenetrable sheath of polymer due to the connectedness of the ionic groups to the polymer chains. As a result, the radius of closest approach, R_{CA}, is greater than R_1. Other parameters obtained from the model analysis are V_p, the total volume of material per ionic aggregate (reciprocal of aggregate number density), and ρ_1. While this model does not predict an upturn in scattered intensity, it does provide better physical rationale for the positional correlation between particles, unlike the high degree of order assumed by the paracrystalline model. To reproduce the entire scattering pattern, another type of scattering entity must be postulated to produce the upturn.

Figures 3 and 4 show the fits of the paracrystalline model to the experimental data, with the parameters determined by nonlinear least squares given in Table I. Figure 3 shows the original data collected 100 eV below the edge, while Figure 4 shows the difference pattern. Part (a) of each figure shows the best fit obtained when only the peak region was considered, while part (b) shows the best fit over the entire range of the SAXS data. Clearly, the paracrystalline model does a poor job of fitting the experimental data. When only the peak region is considered, the model provides a good fit over this region but overpredicts the scattered intensity at low angle. While an underprediction might reflect an experimental artifact such as

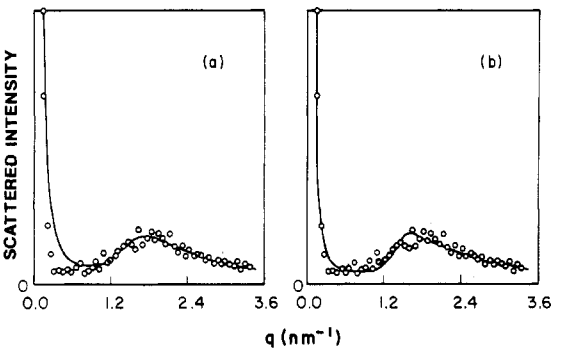

Figure 4. Paracrystalline model fits to difference pattern. (a) Best fit for $0.9 < q < 3.5$ nm^{-1}; (b) best fit for $0.2 < q < 3.5$ nm^{-1}. Solid line is the fit; circles are data.

those discussed previously, or perhaps the presence of unaccounted for scattering intensities, an overprediction clearly points to a faulty model. When the best fit is obtained over the entire data range, the paracrystalline model predicts a much sharper peak than observed, reflecting the unrealistically high degree of order embodied in the model.

We resort then to the modified Yarusso model but must postulate some other type of scattering entity as the origin of the zero-angle upturn. However, assigning the source of this scattering is complicated by the possible presence of dissolved cations in the polystyrene matrix. Yarusso and Cooper[10] have estimated that approximately half the ions in zinc-neutralized sulfonated polystyrene remain outside the ionic aggregates. Therefore, the observed changes in "effective" electron density difference with X-ray energy could result either from a decrease in the scattering power of an ion-rich site relative to the ion-poor matrix or from a decrease in the effective electron density of the matrix relative to regions still poorer in cation, such as voids or crystallites, where present. Thus, both voids and precipitated particles of unreacted nickel acetate, of similar size and number density, could potentially give rise to the observed scattering near zero angle in both the original and difference patterns. Considering the relative amounts of nickel in the aggregates and the matrix, a higher concentration of voids than nickel acetate particles would be required to produce the observed scattering. Yarusso has already shown[34] that a $5/\mu m^3$ concentration of voids of 20 nm in diameter could fit the upturn well. Particles of nickel acetate this size should be readily observable by transmission electron microscopy (TEM), but a comprehensive investigation by Handlin et al.[35] found no such structures; voids of this size may or may not be detected by TEM, depending on sample thickness. Moreover, in Yarusso's experiments,[7,10,34] the upturn was observed for every sulfonated polystyrene ionomer studied, even those where the degree of neutralization was as low as 25%. It seems unlikely that nickel acetate would precipitate in a material with a high concentration of sulfonic acid groups or that voids of a reproducible number and size should be present in every sample.

Another possible source of the zero-angle scattering is an inhomogeneous distribution of the dissolved cations, as shown schematically in Figure 5. To model this possibility, we have employed the Debye–Bueche random-two-phase model.[5,36,37] Here, the heterogeneities follow the correlation function

$$\gamma_0(r) = \exp(-r/c) \tag{7}$$

The constant c is a correlation length, reflecting the average size of the heterogeneities, while r is the radial distance from any point in the material. The scattered in-

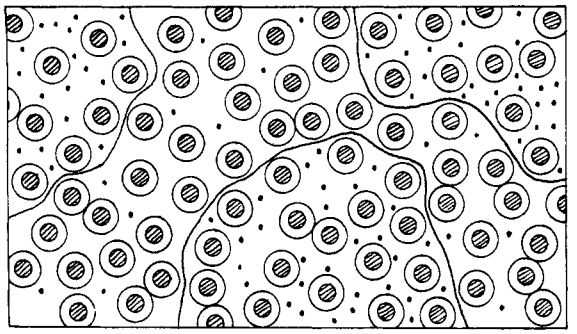

Figure 5. Possible model for the source of zero-angle scattering. Dots represent dissolved cations. Solid line boundaries are drawn to aid in visualizing the inhomogeneous distribution of dissolved cations.

Table II
Combined Modified Yarusso and Debye-Bueche Model Fit Parameters[a]

scattering pattern	R_1, nm	R_{CA}, nm	V_p, nm^3	ρ_1	$\phi_1\phi_2(\Delta\rho)^2$	c, nm
original (100 eV below edge)	0.76	1.57	76.	7.6	0.002	90
difference[b]	0.67	1.57	76.	11.0	0.001	300

[a] Relative values for ρ_1 and $\Delta\rho$, as discussed in text. [b] Difference pattern scaled to match original pattern in integrated intensity.

tensity predicted by this model is obtained by Fourier transformation:[37]

$$I/I_eV = \phi_1\phi_2(\Delta\rho)^2 \int_0^\infty \gamma_0(r)4\pi r^2[\sin(qr)/qr]\,dr = 8\pi\phi_1\phi_2(\Delta\rho)^2/c(q^2 + c^{-2})^2 \quad (8)$$

Here, v is the scattering volume, $\Delta\rho$ is the electron density difference between the ion-rich and ion-poor regions in the material, and ϕ_1 and ϕ_2 are the volume fractions of the two types of regions. Clearly this expression produces a monotonically decreasing scattered intensity with q, so appropriate values of c and $\Delta\rho$ should produce a good fit to the ASAXS data in the upturn region.

Fits to the ASAXS data of the above expression, combined with the modified Yarusso model already discussed, are shown in Figures 6 (for the data 100 eV below the edge) and 7 (difference pattern), with the parameters given in Table II. Considering the noise level in the difference pattern, the Yarusso model parameters are essentially the same for the two fits. The values of the correlation length, c, differ considerably between the original and difference patterns. However, an accurate determination of $\Delta\rho$ and c is complicated by the fact that the upturn is very steep, and thus it is difficult to reliably regress two correlated parameters from the data. It is worth noting that a similar analysis of small-angle neutron scattering data from ampholytic styrene ionomers by Clough et al.[38] yielded a good fit with correlation lengths of 30–40 nm. To obtain a precise value of c, data with an extremely low noise level and properly corrected for any instrumental smearing effects that become important at the lowest angles will be necessary.

Since we do not know the volume fractions of the two types of heterogeneity, a definitive value of $\Delta\rho$ cannot be obtained. However, the $\phi_1\phi_2$ product has its maximum value when the two volume fractions are equal, which allows us to calculate a lower bound on $\Delta\rho$. Assuming that both types of heterogeneity are present in equal amounts, we calculate that $\Delta\rho$ is less than 1% of ρ_1, the electron density difference between the ionic aggregates and the matrix. Therefore, the electron density difference required

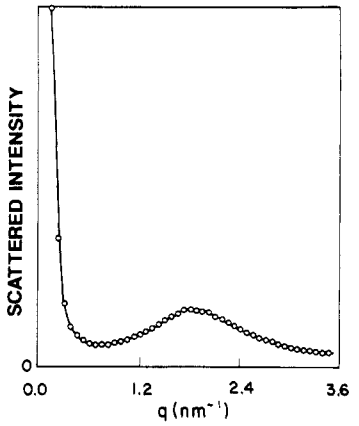

Figure 6. Combined modified Yarusso and Debye–Bueche model fit to the SAXS pattern 100 eV below the nickel K edge. Solid line is the fit, circles are data.

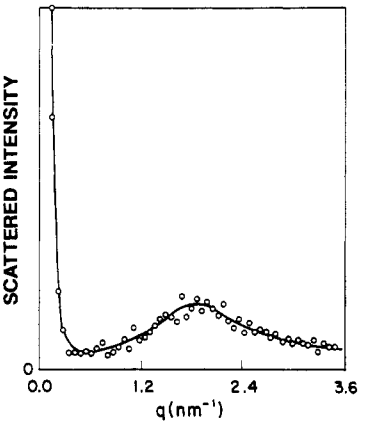

Figure 7. Combined modified Yarusso and Debye–Bueche model fit to the difference pattern. Solid line is the fit; circles are data.

to produce the observed zero-order scattering is very small, while the correlation distance is very large (2 orders of magnitude greater than the diameter of an ionic aggregate). Such a small electron density difference would not be detectable by electron microscopy, in contrast to precipitated nickel acetate or voids.

In all fairness, however, it should be conceded that the Debye–Bueche model is not the only possible explanation for the upturn. Any sort of attractive potential between ionic aggregates will produce an upturn; for example, a similar upturn is observed in SAXS data from liquid and high-pressure gaseous argon,[39] where van der Waals forces provide the attraction. Because of the steepness of the upturn, it is difficult to discriminate between models on the basis of their quality of fit. Based on the preliminary results reported here, we have recently collected a much larger body of ASAXS data from a variety of nickel-neutralized ionomers and hope to shed further light on these issues in a forthcoming paper.

V. Conclusions

The application of anomalous SAXS to ionomers has been demonstrated. Our results indicate that the ubiquitous zero-order scattering is related to the neutralizing cation and may be caused by an inhomogeneous distribution of isolated ionic groups in the material. Application of the Debye–Bueche random-two-phase model to the data indicates that a correlation length of order 100 nm, with an electron density difference less than 1% of the aggregate-matrix contrast, can rationalize the data.

Acknowledgment. We thank Dr. Robert Lundberg and the late Dr. Henry Makowski of Exxon Research and

Engineering Co. for providing the sulfonated polystyrene ionomer. Thanks are also due to Philip E. Gibson for suggesting the Debye–Bueche model and to Soichi Wakatsuki for help with the ASAXS experiments. This work was supported by the U.S. Department of Energy under Contract DE-FG02-84ER45111. R.A.R. wishes to thank S.C. Johnson & Son and the Fannie and John Hertz Foundation for support. The Stanford Synchrotron Radiation Laboratory is supported by the Department of Energy, Office of Basic Energy Sciences, and the National Institutes of Health, Biotechnology Resources Program, Division of Research Resources.

References and Notes

(1) Wilson, F. C.; Longworth, R.; Vaughan, D. J. *Polym. Prepr. (Am. Chem. Soc., Div. Polym. Chem.)* **1968**, *9*, 505.
(2) Marx, C. L.; Caulfield, D. F.; Cooper, S. L. *Macromolecules* **1973**, *6*, 344.
(3) Fujimura, M.; Hashimoto, T.; Kawai, H. *Macromolecules* **1981**, *14*, 1309.
(4) Weiss, R. A.; Lefelar, J. A. *Polymer* **1986**, *27*, 3.
(5) Williams, C. E.; Russell, T. P.; Jérôme, R.; Horrion, J. *Macromolecules* **1986**, *19*, 2877.
(6) Gierke, T. D.; Munn, G. E.; Wilson, F. C. *J. Polym. Sci., Polym. Phys. Ed.* **1981**, *19*, 1687.
(7) Yarusso, D. J.; Cooper, S. L. *Polymer* **1985**, *26*, 371.
(8) Kumar, S.; Pinéri, M. *J. Polym. Sci., Polym. Lett. Ed.* **1986**, *24*, 1767.
(9) MacKnight, W. J.; Taggart, W. P.; Stein, R. S. *J. Polym. Sci., Polym. Symp.* **1974**, *45*, 113.
(10) Yarusso, D. J.; Cooper, S. L. *Macromolecules* **1983**, *16*, 1871.
(11) Ramaseshan, S., Abrahame, S. C., Eds. *Anomalous Scattering*; International Union of Crystallography: Copenhagen, 1975.
(12) Wagner, C. N. J. *J. Non-Cryst. Solids* **1980**, *42*, 3.
(13) James, R. W. *The Optical Principles of the Diffraction of X-Rays*; Cornell University: Ithaca, NY, 1965.
(14) Phillips, J. C.; Hodgson, K. O. In *Synchrotron Radiation Research*; Winick, H., Doniach, S., Eds.; Plenum: New York, 1980.
(15) Waseda, Y. *Novel Application of Anomalous X-Ray Scattering for Structural Characterization of Disordered Materials*; Springer-Verlag: New York, 1984.
(16) Stuhrmann, H. B. *Adv. Polym. Sci.* **1985**, *67*, 123.
(17) Lye, R. C.; Phillips, J. C.; Kaplan, D.; Doniach, S.; Hodgson, K. O. *Proc. Natl. Acad. Sci. U.S.A.* **1980**, *77*, 5884.
(18) Miake-Lye, R. C.; Doniach, S.; Hodgson, K. O. *Biophys. J.* **1983**, *41*, 287.
(19) Fairclough, R. H.; Miake-Lye, R. C.; Stroud, R. M.; Hodgson, K. O.; Doniach, S. *J. Mol. Biol.* **1986**, *189*, 673.
(20) Makowski, H. S.; Lundberg, R. D.; Singhal, G. H. U.S. Patent 3 870 841, 1975, to Exxon Research and Engineering Co.
(21) Lundberg, R. D.; Makowski, H. S.; Westerman, L. U.S. Patent 4 014 847, 1977, to Exxon Research and Engineering Co.
(22) Hubbard, S. R. Ph.D. Thesis, Stanford University, 1987.
(23) Bonse, U.; Hartmann-Lotsch, I. *Nucl. Instrum. Methods Phys. Res., Sect. A* **1984**, *222*, 185.
(24) Kronig, R. de L. *J. Opt. Soc. Am. Rev. Sci. Instrum.* **1926**, *12*, 527.
(25) Kramers, H. A. *Atti Congr. Fisici*, Como **1927**, 545.
(26) Suortti, P.; Hastings, J. B.; Cox, D. E. *Acta Crystallogr., Sect. A: Found. Crystallogr.* **1985**, *A41*, 417.
(27) Aur, S.; Kofalt, D.; Waseda, Y.; Egami, T.; Chen, H. S.; Teo, B.-K.; Wang, R. *Nucl. Instrum. Methods Phys. Res., Sect. A* **1984**, *222*, 259.
(28) Hosemann, R.; Bagchi, S. N. *Direct Analysis of Diffraction by Matter*; North-Holland: Amsterdam, 1962.
(29) Percus, J. K.; Yevick, G. *Phys. Rev.* **1958**, *110*, 1.
(30) Wertheim, M. S. *Phys. Rev. Lett.* **1963**, *10*, 321.
(31) Thiele, E. *J. Chem. Phys.* **1963**, *39*, 474.
(32) Fournet, G. *Acta Crystallogr.* **1951**, *4*, 293, 587.
(33) Kinning, D. J.; Thomas, E. L. *Macromolecules* **1984**, *17*, 1712.
(34) Yarusso, D. J. Ph.D. Thesis, University of Wisconsin—Madison, 1983.
(35) Handlin, D. L.; MacKnight, W. J.; Thomas, E. L. *Macromolecules* **1981**, *14*, 795.
(36) Debye, P.; Bueche, A. M. *J. Appl. Phys.* **1949**, *20*, 518.
(37) Debye, P.; Anderson, H. R.; Brumberger, H. *J. Appl. Phys.* **1957**, *28*, 679.
(38) Clough, S. B.; Cortelek, D.; Nagabhushanam, T.; Salamone, J. C.; Watterson, A. C. *Polym. Eng. Sci.* **1984**, *24*, 385.
(39) Eisenstein, A.; Gingrich, N. S. *Phys. Rev.* **1942**, *62*, 261.

Neutron and X-ray Scattering Studies on Semicrystalline Polymer Blends

T. P. Russell* and H. Ito

IBM Research, Almaden Research Center, 650 Harry Road, San Jose, California 95120-6099

G. D. Wignall

Oak Ridge National Laboratory, Oak Ridge, Tennessee 37830.
Received September 19, 1987; Revised Manuscript Received December 8, 1987

ABSTRACT: Mixtures of poly(ethylene oxide), PEO, with protonated or deuteriated poly(methyl methacrylate), PMMAH or PMMAD, respectively, crystallized at 50 °C have been investigated by small-angle X-ray scattering, SAXS, and small-angle neutron scattering, SANS. It is shown that PMMA is incorporated into the amorphous phase between the crystalline lamellae. In addition, the thickness of the crystalline lamellae remains constant as a function of temperature which is in keeping with a small interaction parameter between the PEO and PMMA. The diffuse-phase boundary between the crystalline and amorphous phase is ca. 15 Å greater for the SAXS measurements than that measured by SANS. These results suggest the existence of a region on the crystal surface in which the crystalline order dissipates and from which the noncrystallizable PMMA is excluded.

Introduction

The morphology in mixtures of semicrystalline and amorphous polymers develops from a balance between kinetic and thermodynamic factors. In particular, the rate of crystal growth will depend upon the temperature at which the crystallization occurs in relation to the glass transition temperature and the equilibrium melting point. In the case of mixtures, the specific interactions between the two polymers and the cooperative diffusion coefficient will also play key roles in the development of the morphology. For example, the amorphous component in mixtures of semicrystalline and amorphous polymers can reside between the crystalline lamellae or be excluded from the interlamellar amorphous phase yet be incorporated within the spherulitic structure or even be rejected, partially or completely, from the spherulite forming a matrix in which the spherulites are embedded. The first case has been clearly demonstrated with mixtures of poly(ϵ-caprolactone) with poly(vinyl chloride)[1] and poly(vinylidine fluoride), PVF_2, with poly(methyl methacrylate), PMMA,[2]

0024-9297/88/2221-1703$01.50/0